Biophysical Chemistry 19 (1984) 25–37
Elsevier

BPC 00823

FLUORESCENCE DECAY STUDIES OF THE DNA-3,6-DIAMINOACRIDINE COMPLEXES

Yukio KUBOTA, Yuko MOTODA, Yuki KUROMI and Yasuo FUJISAKI

Department of Chemistry, Faculty of Science, Yamaguchi University, Yamaguchi 753, Japan

Received 1st May 1983
Accepted 24th August 1983

Key words: DNA-aminoacridine complex; Nanosecond pulse fluorometry; Fluorescence lifetime

The interaction of several 3,6-diaminoacridines with DNAs of various base composition has been studied by steady-state and transient fluorescence measurements. The acridine dyes employed are of the following two classes: class I – proflavine, acriflavine and 10-benzyl proflavine; class II – acridine yellow, 10-methyl acridine yellow and benzoflavine. It is found that the fluorescence decay kinetics follows a single-exponential decay law for free dye and the poly[d(A-T)]-dye complex, while that of the dye bound to DNA obeys a two-exponential decay law. The long lifetime (τ_1) for each complex is almost the same as the lifetime for the poly[d(A-T)]-dye complex, and the amplitude α_1 decreases with increasing GC content of DNA. The fluorescence quantum yields (Φ_F) of dye upon binding to DNA decrease with increasing GC content; the Φ_F values for class I are nearly zero when bound to poly(dG)·poly(dC), but those for class II are not zero. This is in harmony with the finding that GMP almost completely quenches the fluorescence for class I, whereas a weak fluorescence arises from the GMP-dye complex for class II. The fluorescence spectra of the DNA-dye complexes gradually shift toward longer wavelengths with increasing GC content. In this connection, the fluorescence decay parameters show a dependence on the emission wavelength; α_1 decreases with an increase in the emission wavelength. In view of these results, it is proposed that the decay behavior of the DNA-dye complexes has its origin in the heterogeneity of the emitting sites; the long lifetime τ_1 results from the dye bound to AT-AT sites, while the short lifetime τ_2 is attributable to the dye bound in the vicinity of GC pairs. Since GC pairs almost completely quench the fluorescence for class I, partly intercalated or externally bound dye molecules may play an important role in the component τ_2.

1. Introduction

Since many of the acridine derivatives have important biological activities, acting as mutagens, carcinogens and bacteriostatic agents, the interaction between DNA and various acridines has been extensively studied [1–4]. The binding data for acridine dyes with DNA have shown that there are two distinct binding modes which correspond to strong and weak binding [1,5]. It is well recognized that the strong binding mode which predominates at a high molar ratio of DNA phosphate to dye (P/D) corresponds to intercalation between adjacent base-pairs [6,7]. This model rationalizes the biological activity of certain acridine dyes acting as mutagens [8,9].

9-Aminoacridine (9AA) and proflavine (PF) are typical acridine dyes that bind to DNA and possess strong mutagenic activity [10]. Fluorescence quantum yield measurements of the DNA-9AA and DNA-PF complexes have revealed that there are two categories of strong binding sites, emitting and quenching sites, and that GC base-pairs or guanine residues are responsible for the quenching sites [11–17]. Very recently, we have found that the fluorescence decay kinetics of the DNA-9AA complex is dependent on the GC content of DNA and obeys a three-exponential decay law, suggesting that the emitting sites of 9AA on DNA consist of at least three classes [17].

The heterogeneity of binding sites or specific interactions between the dye and DNA bases may be important for the understanding of the biological actions of acridines dyes [14,18,19]. Accord-

ingly, it is of great interest to study in detail the fluorescence decay behavior of 3,6-diaminoacridine derivatives such as PF and acridine yellow (AY) when complexed with DNA or GMP and to compare the results with those of 9AA. In the present study, six 3,6-diaminoacridine derivatives have been examined. It was found, in contrast with the results of 9AA, that the fluorescence decay kinetics for each dye upon binding to DNA obeyed a two-exponential decay law, and possible interpretations are discussed.

2. Experimental

2.1. Materials

The following DNAs and synthetic polynucleotides were commercial products: *Clostridium perfringens* DNA (Worthington), calf thymus DNA (Worthington), *Escherichia coli* DNA (Worthington), *Micrococcus lysodeikticus* DNA (Miles), poly[d(A-T)] (Miles) and poly(dG) · poly(dC) (Miles). GMP, chromatographically pure, was purchased from Sigma Chemical Co. or Seikagaku Kogyo. The following two classes of 3,6-diaminoacridine derivatives were used: class I – PF (3,6-diaminoacridine; British Drug Houses), acriflavine (3,6-diamino-10-methylacridinium chloride, AF; Chroma) and 3,6-diamino-10-benzylacridinium chloride (PF-BZ); class II – AY (3,6-diamino-2,7-dimethylacridine; Chroma), 3,6-diamino-2,7-dimethyl-10-methylacridinium chloride (AY-ME) and benzoflavine (3,6-diamino-2,7-dimethyl-9-phenylacridine, BF; Chroma). PF-BZ and AY-ME were prepared according to the method of Browning et al. [20] and the method of Ullmann and Marić [21], respectively. All dyes were purified by repeated crystallization and chromatography. Any trace of impurity was not detected by the method of thin-layer chromatography for each dye. 1,1,4,4-Tetraphenyl-1,3-butadiene (TPB), purchased from Tokyo Kasei, was twice recrystallized from benzene. Spectral grade cyclohexane was obtained from Wako Jyunyaku. Other chemicals were of reagent grade purity or better. Glass-redistilled water was used for the preparation of all aqueous solutions.

2.2. Absorption and fluorescence spectra

Absorption and steady-state fluorescence spectra were recorded with a Shimadzu UV-200S spectrophotometer and a Hitachi MPF-2A spectrophotofluorometer, respectively. Observed fluorescence spectra were corrected for the unequal quantum response of the detector system which consists of lenses, a monochromator and an R106-UH or an R446-UR photomultiplier tube (Hamamatsu TV). Fluorescence quantum yields were determined by comparing the area under the spectrum of the DNA-dye complex with the corresponding area of PF and by taking 0.44 for the quantum yield of PF [13,16].

2.3. Fluorescence decay curves

Transient fluorescence decay curves were measured with an Ortec time-resolved emission spectrophotometer [17]. Excitation pulses from a flashlamp were passed through a Corning 7-60 filter or a 400-nm interference filter (Vacuum Optics Corp., Japan) and focused on the sample with a lens. The emission was observed by an RCA 8850 photomultiplier tube through a grating monochromator (Applied Photophysics Ltd.), the half-bandwidth being 5–20 nm according to the fluorescence intensity of the sample. To avoid interfering effects due to decay of emission anisotropy [22], the excitation was done with an unpolarized beam of light and the emission was observed through a Polacoat polarizer whose axis was 54.7° to the excitation observation plane. The observed fluorescence decay $i(t)$ is represented by the convolution integral:

$$i(t) = \int_0^t g(u)\, I(t-u)\,\mathrm{d}u \qquad (1)$$

where $g(t)$ is the apparatus response function and $I(t)$ the fluorescence decay which would have been obtained with the δ-pulse excitation. The apparatus response function $g(t)$ was determined from the fluorescence decay curve of TPB in deaerated cyclohexane which has a single-exponential decay ($\tau = 1.7$ ns at 25°C) [17]. Deconvolution of eq. 1 was made with the aid of the method of nonlinear least squares [23] and/or the method of Laplace

transformation [24] by assuming that $I(t)$ is a sum of exponential functions:

$$I(t) = \sum_{i=1}^{n} \alpha_i \exp(-t/\tau_i) \quad (2)$$

where α_i and τ_i are the amplitude and lifetime, respectively, of the i-th component. Goodness of fit between observed and theoretical decay curves was judged by inspection of the reduced χ^2, the weighed residuals and the autocorrelation function of the residuals [23–25]. Data analysis was accomplished with a PDP 11/04 minicomputer (Digital Equipment Corp.) interfaced with an Ortec 6240B multichannel analyzer.

All measurements were carried out at 25 ± 0.1°C in 5 mM phosphate buffer (pH 6.9) unless otherwise stated. Dye concentrations were in the range 1.0–5.1 μM.

3. Results

3.1. Absorption and fluorescence spectra

Figs. 1 and 2 show the absorption spectra of the calf thymus DNA-PF-BZ and *C. perfringens* DNA-AY systems, respectively, as a function of P/D. The absorption bands can be seen to shift progressively toward a limit (curve 7 in fig. 1 and curve 9 in fig. 2) which represents the spectrum of the dye in a fully complexed form. In the case of PF-BZ, all the curves pass through an isosbestic point (465 nm), indicating that they result from the contributions of two forms of PF-BZ, free and bound, each form having a characteristic absorption spectrum. Very similar absorption changes were also obtained with PF and AF complexed with various DNAs.

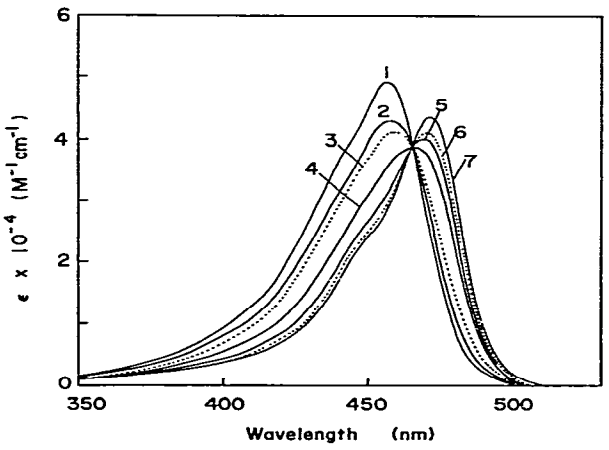

Fig. 1. Absorption spectra of the calf thymus DNA-PF-BZ system in 5 mM phosphate buffer (pH 6.9) at 25°C. PF-BZ: 5.1 μM. P/D: (1) 0, (2) 1.0, (3) 2.0, (4) 4.0, (5) 8.0, (6) 15.1, (7) 47.8.

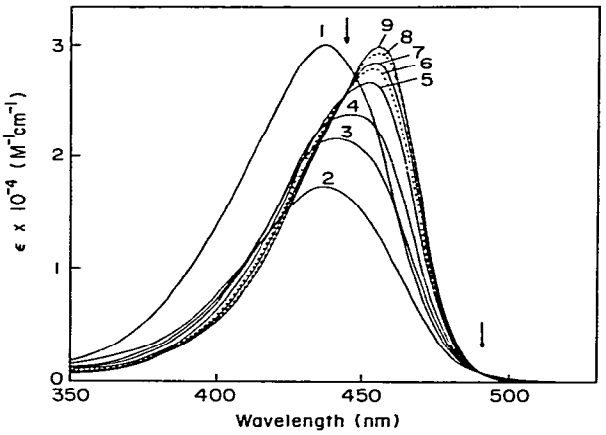

Fig. 2. Absorption spectra of the *C. perfringens* DNA-AY system in 5 mM phosphate buffer (pH 6.9) at 25°C. AY: 5.0 μM. P/D: (1) 0, (2) 1.0, (3) 2.0, (4) 3.1, (5) 5.1, (6) 7.2, (7) 10.3, (8) 20.5, (9) 30.8. The arrows indicate isosbestic points for the absorption spectra of the bound AY in which the contribution of the free dye has been subtracted.

In contrast to class I, the absorption bands for class II showed no clear isosbestic points. As fig. 2 illustrates typical absorption changes obtained with the *C. perfringens* DNA-AY system, the monomer band at 455 nm is depressed and its maximum shifts toward shorter wavelengths with decreasing P/D value. On the other hand, the absorption spectra of the bound AY where the contribution of the free dye has been subtracted displayed isosbestic points (445 and 490 nm) provided that the ratio of the bound dye to DNA phosphate did not exceed about 0.2 (fig. 2). This finding suggests that the bound AY is transformed gradually from one type of complex (complex I) at a high P/D value

to a different type of complex (complex II) at a low P/D value. Very similar absorption spectra were also observed with the DNA-AY-ME and DNA-BF systems. In analogy with the DNA-acridine orange system [26–28], complex I may be attributed to an intercalated monomeric dye, while complex II may be ascribed to a bound dye dimer. In view of the finding that the dimerization equilibrium constant of AY (1.05×10^4 M^{-1}) was much larger than that of PF (1.5×10^3 M^{-1}), the tendency of self-association of the dye may be responsible for the distinction of between the absorption spectral behavior of class I and II. Further details will be presented elsewhere.

In order to avoid complication due to the presence of different binding processes, the following fluorescence studies were performed at sufficiently high P/D values (P/D > 100) where complex I predominates and the concentration of the free dye is negligibly small.

Figs. 3 and 4 depict the steady-state fluorescence spectra of PF and AY, respectively, in the presence of various DNAs at high P/D values. The shape and the maximum of the fluorescence spectrum of each dye bound to DNA are dependent on the GC content of DNA. A blue shift and a narrowing of the fluorescence band are observed upon binding to DNA as compared to the spectrum of the free dye. As can be seen in figs. 3 and 4, there is a red shift of the fluorescence band with increasing GC content. This behavior was more pronounced in the case of class II than class I in which the magnitude of spectral shifts was in the order: PF-BZ > AF > PF. Similarly, the absorption spectra of the bound dye show only a slight dependence on the GC content; there is a blue shift of the spectrum with increasing GC content. The spectral behavior of the bound PF agrees with that previously reported [15].

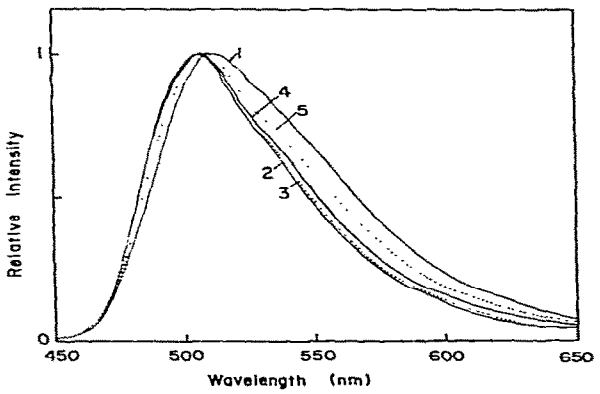

Fig. 3. Normalized fluorescence quantum spectra of PF (5.0 μM) in the presence of various DNAs in 5 mM phosphate buffer (pH 6.9) at 25°C: (1) free, (2) poly[d(A-T)] (P/D = 108) and *C. perfringens* DNA (P/D = 200), (3) *E. coli* DNA (P/D = 399), (4) *M. lysodeikticus* DNA (P/D = 200), (5) poly(dG)·poly(dC) (P/D = 101). The excitation wavelength was 400 nm.

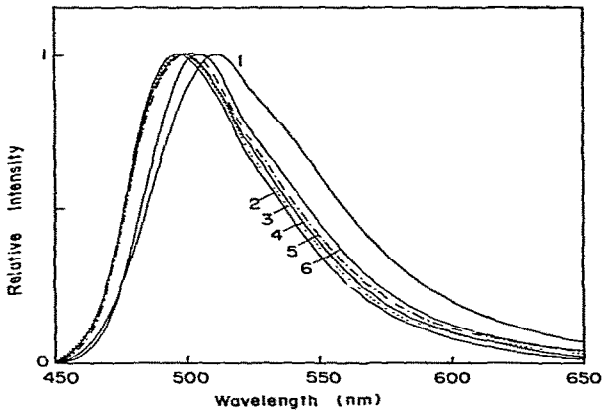

Fig. 4. Normalized fluorescence quantum spectra of AY (5.0 μM) in the presence of various DNAs in 5 mM phosphate buffer (pH 6.9) at 25°C: (1) free, (2) poly[d(A-T)] (P/D = 108), (3) *C. perfringens* DNA (P/D = 200), (4) calf thymus DNA (P/D = 799), (5) *M. lysodeikticus* DNA (P/D = 400), (6) poly(dG)·poly(dC) (P/D = 101). The excitation wavelength was 400 nm.

3.2. Fluorescence quantum yields

The fluorescence quantum yield (Φ_F) of the dye bound to DNA strongly depended on its base composition. As can be seen in fig. 5, the Φ_F value decreases with increasing GC content. This trend for PF and AF is consistent with that previously reported [11–13,15,16,29]. The Φ_F value of the poly(dG)·poly(dC)-dye complex for class I is nearly zero, while that for class II is not zero (table 1). This result suggests that a GC pair almost

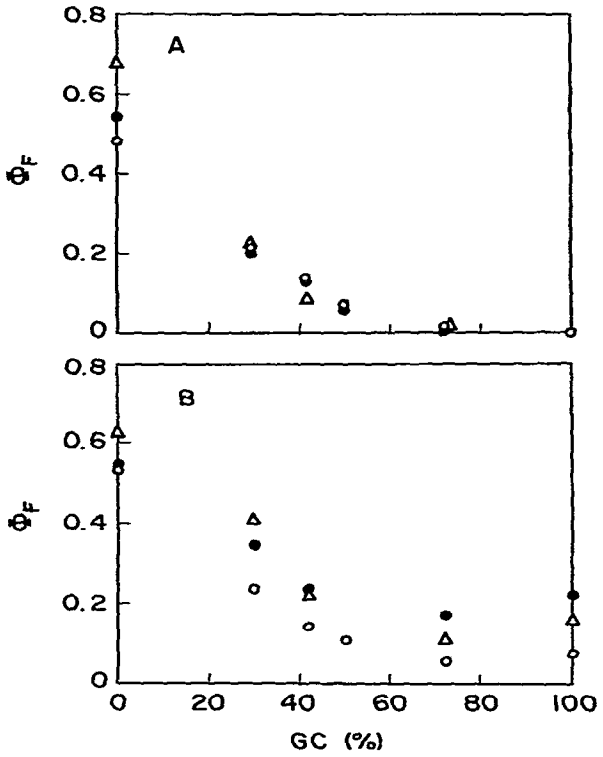

Fig. 5. Fluorescence quantum yields (Φ_F) of the DNA-dye complexes vs. the GC content of DNA. (A) PF (○), AF (●), PF-BZ (△). (B) AY (○), AY-ME (●), BF (△).

completely quenches the fluorescence for class I, whereas the dye bound in the vicinity of GC pairs is still fluorescent for class II although its fluorescence is markedly quenched.

3.3. Fluorescence decay curves

Since the fluorescence quantum yield of the bound dye shows a strong dependence on the GC content of DNA, transient fluorescence decay curves were measured for further investigating the interaction of the dye with the binding sites. Decay measurements were made at high P/D values (P/D > 100) and at low ionic strength (5 mM phosphate buffer) to minimize the effects of unbound dye and energy transfer [30]. Under these conditions, the contribution of the free dye was estimated to be below 0.2% on the basis of equilibrium dialysis data (Kubota et al., unpublished results).

It was found that the fluorescence decay kinetics of the dye followed a single-exponential decay law but that of the dye bound to DNA was complex. Typical decay curves obtained with the calf thymus DNA-AY and *M. lysodeikticus* DNA-AY complexes are shown in figs. 6 and 7, respectively. Both figures indicate that the decay kinetics of AY upon binding to DNA obeys a two-exponential decay law. It was also found that all

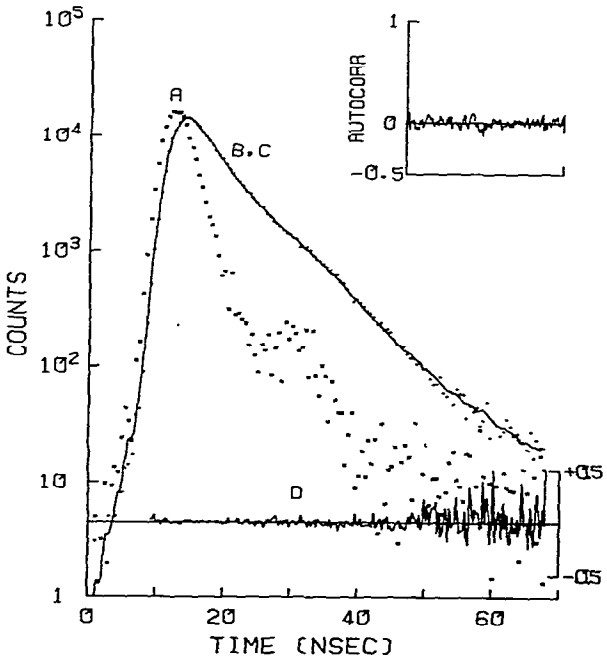

Fig. 6. Two-component analysis of the fluorescence decay of the calf thymus DNA-AY complex (P/D = 799) in 5 mM phosphate buffer (pH 6.9) at 25°C. The concentration of AY was 5.0 μM, and the decay was observed at 495 nm. Curve A is the apparatus response function. Curve B is the observed decay curve. The smooth curve C shows the best theoretical decay curve based on two exponentials. Curve D is the weighed residuals. The inset is the autocorrelation function of the residuals. Parameters obtained: $\tau_1 = 6.8$ ns, $\tau_2 = 1.5$ ns, $\alpha_1 = 0.150$, $\alpha_2 = 0.384$ and $\chi^2 = 1.64$. The amplitudes normalized to unity are $\alpha_1 = 0.28$ and $\alpha_2 = 0.72$.

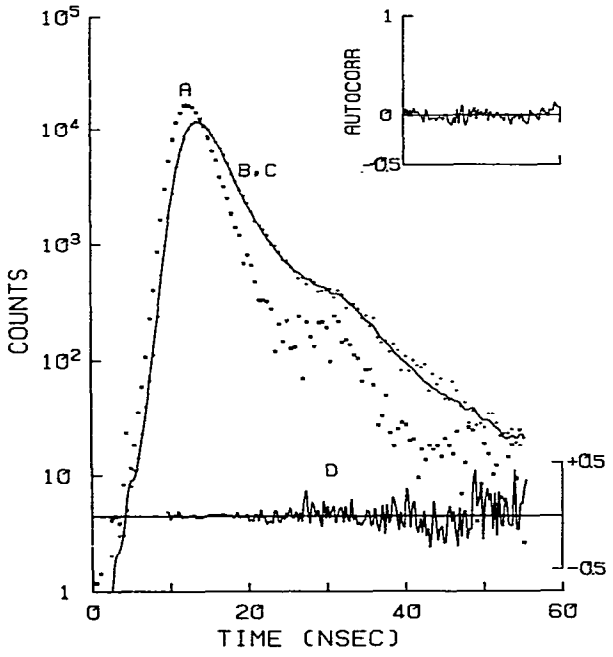

Fig. 7. Two-component analysis of the fluorescence decay of the *M. lysodeikticus* DNA-AY complex (P/D = 400) in 5 mM phosphate buffer (pH 6.9) at 25°C. Conditions and legends to each curve are as described for fig. 6. The theoretical decay curve is based on the following parameters: $\tau_1 = 6.9$ ns, $\tau_2 = 1.2$ ns, $\alpha_1 = 0.032$, $\alpha_2 = 0.583$ and $\chi^2 = 1.58$. The amplitudes normalized to unity are $\alpha_1 = 0.05$ and $\alpha_2 = 0.95$.

decay curves could be well described as a sum of two exponentials except for the *C. perfringens* DNA-PF and calf thymus DNA-PF complexes in which one-component analysis gave the best results. Typical sets of the decay parameters obtained for the DNA-dye complexes at high P/D values are summarized in table 1. As shown by the results for the DNA-AY complexes in table 1, P/D (P/D > 100) and ionic strength (I = 0.01–0.31) did not affect the decay parameters. This finding suggests that the decay parameters presented here are characteristic of the dye bound to DNA.

It can be clearly seen from table 1 that the decay parameters, especially the amplitudes, depend on both the base composition of DNA and the dye structure. On the other hand, Duportail et al. [31] have reported that the fluorescence decays of several acridine dyes (PF, 9AA, etc.) can be resolved into two components corresponding to a short and a long lifetime and that relative proportions of these two components depend only slightly on the DNA base composition, but do not depend on the dye structure. There is a significant disagreement between our work and the results of Duportail et al. [31]. However, their results should be reexamined because they did not take into account artifacts, anisotropic contributions to the observed decay [22] and energy-dependent effects of the photomultiplier tube [32], which might introduce significant errors in determination of the decay parameters.

3.4. Fluorescence decays of poly[d(A-T)]-dye and poly(dG)·poly(dC)-dye complexes

We next examined the fluorescence decays of the dye upon binding to poly[d(A-T)] and poly(dG)·poly(dC) which contain only one type of binding site. As shown by the typical decay curves obtained with the poly[d(A-T)]-AY complex in fig. 8, it was found that the fluorescence decay of the dye bound to poly[d(A-T)] followed a single-exponential decay law. It is to be noted that for each dye the component τ_1 of the DNA-dye complex is almost the same as the lifetime of the poly[d(A-T)]-dye complex (table 1). On the other hand, the fluorescence decay of the dye bound to poly(dG)·poly(dC) was found to obey a two-exponential decay law. The decay behavior, shown in table 1, differs between class I and II. The amplitude α_1 is much smaller than the amplitude α_2 in the case of class I, but both amplitudes are almost of the same magnitude in the case of class II. In harmony with the Φ_F values obtained for the dye upon binding to poly(dG)·poly(dC) (table 1), this result also implies that quenching interactions between the dye and the GC pair are different for class I and II.

3.5. Dependence of decay parameters on emission wavelength

Since the fluorescence spectrum of the dye upon binding to DNA depends on the base composi-

Table 1

Fluorescence decay parameters and quantum yields for PF, AF, PF-BZ, AY, AY-ME, BF and their complexes with DNAs of various base composition

The solvent was 5 mM phosphate buffer (pH 6.9) at 25°C, and the dye concentration was 5.0–5.1 μM. The emission was observed at 500 nm for free dyes and poly(dG)·poly(dC)-dye complexes and at 495 nm for the other systems. χ^2 values ranged from 1.1 to 1.9. The amplitudes (α values) are normalized to unity.

System	GC(%)	P/D	τ_1 (ns)	α_1	τ_2 (ns)	α_2	Φ_F
PF							
Free			4.8	1.00			0.440
Poly[d(A-T)]	0	108	6.7	1.00			0.477
C. perfringens DNA [a]	30	408	6.3	1.00			0.211
Calf thymus DNA [a]	42	400	6.4	1.00			0.141
E. coli DNA	50	399	6.5	0.78	1.8	0.22	0.066
M. lysodeikticus DNA	72	400	6.1	0.18	0.4	0.82	0.017
Poly(dG)·poly(dC) [b]	100	101	6.0	0.008	0.5	0.992	0.005
AF							
Free			5.0	1.00			0.547
Poly[d(A-T)]	0	108	5.5	1.00			0.544
C. perfringens DNA	30	200	5.4	0.87	1.7	0.13	0.200
Calf thymus DNA	42	400	5.4	0.79	1.4	0.21	0.131
E. coli DNA	50	200	5.4	0.65	1.3	0.35	0.055
M. lysodeikticus DNA	72	200	4.8	0.18	0.4	0.82	0.013
Poly(dG)·poly(dC) [c]	100	108	5.2	0.006	0.5	0.994	0.017
PF-BZ							
Free			4.8	1.00			0.601
Poly[d(A-T)]	0	104	5.3	1.00			0.683
C. perfringens DNA	30	221	5.0	0.78	2.0	0.22	0.230
Calf thymus DNA	42	406	4.8	0.62	1.4	0.38	0.080
M. lysodeikticus DNA	72	218	4.2	0.23	0.5	0.77	0.018
Poly(dG)·poly(dC) [c]	100	109	5.1	0.07	0.5	0.93	0.013
AY							
Free			5.2	1.00			0.424
Poly[d(A-T)]	0	108	6.9	1.00			0.532
C. perfringens DNA	30	407	6.9	0.49	1.6	0.51	0.235
		200	6.8	0.50	1.4	0.50	0.250
Calf thymus DNA	42	799	6.8	0.28	1.5	0.72	0.137
		400	6.7	0.27	1.5	0.73	0.142
		400 [d]	6.9	0.28	1.5	0.72	0.128
		400 [e]	6.9	0.28	1.5	0.72	0.141
		400 [f]	6.9	0.27	1.3	0.73	0.142
E. coli DNA	50	400	6.9	0.24	1.5	0.76	0.108
		200	6.7	0.24	1.4	0.76	0.108
M. lysodeikticus DNA	72	400	6.9	0.05	1.2	0.95	0.052
		200	6.6	0.05	1.2	0.95	0.052
Poly(dG)·poly(dC) [b]	100	101	4.8	0.39	1.3	0.61	0.070
AY-ME							
Free			4.8	1.00			0.440
Poly[d(A-T)]	0	102	5.5	1.00			0.541
C. perfringens DNA	30	219	5.5	0.50	1.8	0.50	0.350
Calf thymus DNA	42	229	5.1	0.35	1.8	0.65	0.235
M. lysodeikticus DNA	72	216	4.3	0.28	1.3	0.72	0.168
Poly(dG)·poly(dC) [c]	100	109	4.4	0.55	1.2	0.45	0.221

Table 1 (continued)

System	GC (%)	P/D	τ_1 (ns)	α_1	τ_2 (ns)	α_2	Φ_F
BF							
Free			5.3	1.00			0.463
Poly[d(A-T)]	0	105	6.9	1.00			0.624
C. perfringens DNA	30	224	6.8	0.48	1.5	0.52	0.415
Calf thymus DNA	42	233	6.7	0.26	1.4	0.74	0.228
M. lysodeikticus DNA	72	220	6.2	0.06	1.1	0.94	0.112
Poly(dG)·poly(dC) [c]	100	111	4.7	0.54	1.4	0.46	0.165

[a] One-component analysis yielded the best results.
[b] According to the manufacturer (Miles), G = 47% and C = 53%.
[c] G = 41% and C = 59%.
[d] The solvent was 5 mM sodium phosphate, 0.1 M NaCl, pH 6.9, 25°C.
[e] 5 mM sodium phosphate, 0.2 M NaCl, pH 6.9, 25°C.
[f] 5 mM sodium phosphate, 0.3 M NaCl, pH 6.9, 25°C.

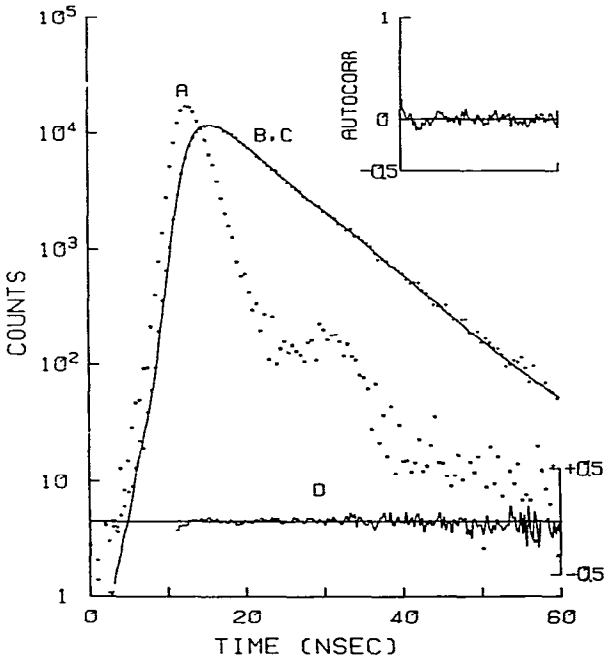

Fig. 8. One-component analysis of the fluorescence decay of the poly[d(A-T)]-AY complex (P/D = 108) in 5 mM phosphate buffer (pH 6.9) at 25°C. Conditions and legends to each curve are as described for fig. 6. The theoretical decay curve is based on the following parameters: $\tau = 6.9$ ns, $\alpha = 0.258$ and $\chi^2 = 1.88$.

tion, it was of interest to study whether or not the decay parameters depend upon the emission wavelength. Typical results obtained with the calf thymus DNA-PF-BZ and calf thymus DNA-AY complexes are summarized in table 2. It is evident that the two lifetimes do not show any significant changes with the emission wavelength, whereas the amplitudes are dependent on it; there is a decrease in α_1 and an increase in α_2 at the longer wavelength (table 2).

3.6. Fluorescence behavior of GMP-dye complexes

In order to understand the nature of interactions between the dye and DNA, the fluorescence properties of the dye complexed with mononucleotides were investigated. Of the four mononucleotides, only GMP caused a strong quenching of the dye fluorescence. The absorption spectra of the dye in the presence of GMP showed a red shift and a decrease in the intensity, as a result of the formation of the specific complex between the dye and GMP [15,33,34]. In the case of class I, the fluorescence and fluorescence-excitation spectra of the dye in the presence of GMP were identical with the corresponding spectra of the free dye. On the other hand, the progressive red shift of the fluorescence spectra with increasing GMP concentration was observed for class II, suggesting that the fluorescence spectrum may be assigned to the superposition of emissions of both the free and

Table 2

Decay parameters obtained for calf thymus DNA-PF-BZ (P/D = 205) and calf thymus DNA-AY (P/D = 204) complexes in 5 mM phosphate buffer (pH 6.9) at 25°C

The concentrations of PF-BZ and AY were 5.0 and 5.1 μM, respectively. χ^2 ranged from 1.2 to 1.8. The amplitudes (α values) are normalized to unity.

System	Emission wavelength (nm)	τ_1 (ns)	α_1	τ_2 (ns)	α_2
Calf thymus DNA-PF-BZ	480	4.7	0.67	1.3	0.33
	495	4.8	0.63	1.4	0.37
	510	4.9	0.61	1.4	0.39
	530	4.8	0.58	1.4	0.42
Calf thymus DNA-AY	480	6.7	0.32	1.6	0.68
	495	6.7	0.28	1.5	0.72
	510	6.7	0.26	1.4	0.74
	530	6.7	0.23	1.4	0.77
	550	6.6	0.22	1.2	0.78

complexed dye. These observations lead to the conclusion that the GMP-dye complex is nonfluorescent for class I, but fluorescent for class II. In practice, the fluorescence quantum yield of the complex (Φ_0'), which was determined by extrapolating the apparent quantum yield to infinite GMP concentration, was found to be zero and nonzero for class I and II, respectively (table 3).

It was found that the fluorescence decays of the GMP-dye systems for class I obeyed a single-exponential decay law, while those for class II followed a two-exponential decay law, reflecting the contribution of the complex to the total fluorescence.

The quenching data were analyzed according to the general reaction mechanism which takes into account complex formation in the ground state as well as in the excited singlet state; details of analysis have been described elsewhere [34]. The bimolecular quenching rate constant (k_q) and the lifetime of the GMP-dye complex (τ_0') were determined from the transient decay data [34], and the results are summarized in table 3. The magnitudes reported for the rate constant k_q are as expected for a diffusion-controlled reaction [35]. On the other hand, the rate constant k_q obtained from the steady-state fluorescence yields was 20–30% larger than that obtained from the transient decay data. This discrepancy may be ascribed to transient effects associated with diffusion [36]. Taking into account transient effects [34], the effective quenching radius (R_0) for the encounter pair between the dye and GMP was estimated to be 9–13 Å; here, R_0 is the distance that the

Table 3

Parameters for fluoresence quenching of PF, AF, PF-BZ, AY, AY-ME and BF by GMP

The solvent was 0.1 M phosphate buffer (pH 6.8) at 25°C, and the dye concentration was in the range 1.0–2.0 μM. Φ_0 and τ_0 are the fluorescence quantum yield and the lifetime of the free dye; Φ_0' and τ_0' are the corresponding quantities for the GMP-dye complex.

	PF	AF	PF-BZ	AY	AY-ME	BF
Φ_0	0.44	0.55	0.60	0.42	0.46	0.46
Φ_0'	0	0	0	0.030	0.053	0.038
τ_0 (ns)	4.9	5.0	4.8	5.4	4.8	5.2
τ_0' (ns)				0.74	1.18	0.71
k_q ($\times 10^{-9}$) ($M^{-1}\,s^{-1}$)	4.19	3.92	3.62	4.07	3.96	3.81

quenching process occurs with a probability of 1. This value is in agreement with the value ($R_0 \simeq 8$ Å) reported for the GMP-PF [33] and GMP-9AA systems [34]. The results obtained here present strong evidence supporting the contention that guanine residues in DNA play a major role in the fluorescence quenching of the bound dye and act in a different way for class I and II.

4. Discussion

The data presented here indicate that the fluorescence decays of 3,6-diaminoacridine derivatives upon binding to poly[d(A-T)] follow a single-exponential decay law but that those of the dye upon binding to DNA are complex. Our present criteria (the reduced χ^2, weighed residuals and autocorrelation function of the residuals) show that the fluorescence decay curves of the DNA-dye complexes can be well resolved into two exponential components.

It is clear from table 1 that each fluorescence lifetime obtained by the two-component analysis is almost independent of the GC content of DNA or only slightly dependent, while the proportion of the amplitudes (α values) shows a marked dependence. It therefore seems reasonable to conclude that the fluorescence decay behavior of the DNA-dye complex is a result of the heterogeneity of the emitting sites. Possible explanation for the two-exponential decay obtained with the DNA-dye complexes may involve two different binding sites, GC and AT sites. As seen in figs. 3 and 4, the shape of the fluorescence spectrum of the bound dye as well as its maximum is dependent on the GC content. A blue shift and a narrowing of the fluorescence band are observed upon binding to DNA as compared to the spectrum of the free dye. The maximum of the fluorescence band can be seen to shift progressively toward longer wavelengths with increasing GC content (figs. 3 and 4). This change suggests that the fluorescence spectrum may be assigned to the superposition of emissions of the dye bound near AT and GC base-pairs. In harmony with the fluorescence spectral behavior, the decay parameters show a dependence on the emission wavelength; the amplitude α_1 decreases with increasing emission wavelength, while the amplitude α_2 increases (table 2). For each dye the long lifetime τ_1 is almost the same as the lifetime of the corresponding poly[d(A-T)]-dye complex (table 1). Furthermore, there is a continuous decrease of the amplitude α_1 with increasing GC content (table 1). On the other hand, the short lifetime τ_2 is not observed for the poly[d(A-T)]-dye complex and is very close to the τ_2 value obtained for the poly(dG)·poly(dC)-dye complex (table 1) or the τ_0' value obtained for the GMP-dye complex (table 3). In view of these results, it seems reasonable to assume that the long lifetime τ_1 is ascribable to the dye bound to AT sites and the short lifetime τ_2 to the dye bound in the neighborhood of GC pairs.

In addition to the fully intercalated complex proposed by Lerman [6,7], the formation of another type of complex is possible. Temperature-jump relaxation studies have shown that PF binds to DNA in two kinetically distinguishable steps [37–40]. In the first step, the dye binds to phosphate groups at the outside by electrostatic attraction in which the dye can only partly overlap the DNA base rings. This externally bound or partly intercalated complex mainly occurs in the GC-rich regions as a precursor of the fully intercalated complex in the final step [38]. The possibility of partial intercalation or external binding stems from X-ray crystallographic and proton magnetic resonance studies of complex formation between aminoacridines and dinucleotides or oligonucleotides [18,41,42]. Further, a red shift of the fluorescence band with increasing GC content (figs. 3 and 4) indicates that the dye bound in the vicinity of GC pairs is to a considerable extent exposed to the surrounding solvent. This presents further evidence for partial intercalation or external binding.

If we do not distinguish AT pairs from TA pairs and GC pairs from CG pairs, there are three types of intercalation sites in DNA: AT-AT, AT-GC and GC-GC sites. Judging from the effective quenching radius ($R_0 \simeq 9$–13 Å) and $\Phi_0' = 0$ for class I (table 3), it is expected that the greater contact between the dye and guanine residues causes the more efficient quenching of fluorescence. For class I, therefore, full intercalation between GC-GC or AT-GC sites may result in

complete quenching of the dye fluorescence. For class II, on the other hand, the nonzero value of Φ_0' (table 3) implies that the dye bound in the vicinity of GC pairs may be still fluorescent independent of the conformational states, full or partial intercalation. If the amplitude α_1 is plotted against the fraction of the AT-AT site (AT^2), we obtain the result shown in fig. 9. There is a good linearity between α_1 and AT^2 in the case of class II. Since the amplitude is proportional to the number of fluorescing molecules [23], this finding indicates that the long lifetime τ_1 is ascribable to the dye intercalated in AT-AT sites, while the short lifetime τ_2 is attributable to the dye bound to AT-GC

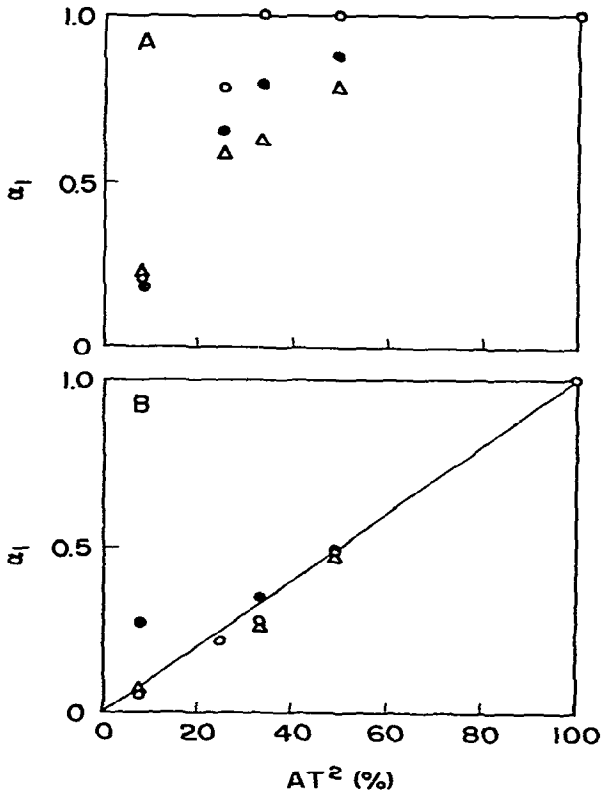

Fig. 9. The amplitude α_1 corresponding to the long lifetime τ_1 vs. the fraction of the AT-AT site (AT^2). (A) PF (○), AF (●), PF-BZ(△). (B) AY (○), AY-ME (●), BF (△).

or GC-GC sites. As inferred from the fluorescence spectral shift (fig. 4), it appears likely that the partly intercalated or externally bound dye plays a major role in the component τ_2. On the other hand, the deviation from linearity for class I (fig. 9) can be understood to show that only the partly intercalated or externally bound dye in AT-GC or GC-GC sites is responsible for the component τ_2; this interpretation is consistent with the zero value of Φ_0' (table 3). As can be seen in fig. 9, the contribution of the component τ_2 appears to increase in the order: PF-BZ > AF > PF. If we assume that preferential binding to particular sites does not occur and bound dye molecules are randomly distributed among the available binding sites [17], we can estimate the proportion of the partly intercalated or externally bound dye, using the equation $\alpha_2 AT^2/\alpha_1(1 - AT^2)$. The values thus obtained are about 0.09 for PF, 0.15 for AF and 0.27 for PF-BZ except for the *M. lysodeikticus* DNA-dye complexes (0.29–0.39). This finding suggests that the introduction of the bulky substituent into the acridine ring may cause the increase in proportion of the partly intercalated or externally bound dye. The single-exponential decays observed for the *C. perfringens* DNA-PF and calf thymus DNA-PF complexes (table 1) may be due to the small proportion of the partly intercalated or externally bound dye.

In the case of class I, the quantum yield of the dye upon binding to poly(dG)·poly(dC) is very low and the component τ_2 is dominant (table 1). The component τ_1 may be due to the unequal content of guanine and cytosine bases in the sample of poly(dG)·poly(dC) or to the contribution of the free dye. In contrast, the corresponding quantum yield for class II is relatively high (table 1). Further, there is a considerable contribution of the component τ_1, suggesting the presence of two different forms of the complex (table 1). This result is particularly surprising in view of the strong quenching ability of GC pairs or guanine residues. This cannot be explained solely by a slight excess of cytosine in the sample of poly(dG)·poly(dC) examined. It may be that the presence of the methyl groups at the 2,7-positions of the acridine ring produces some structural changes at the binding sites in such a way that the bound dye be-

comes fluorescent; however, this is still not clear from the present work.

The data presented in this paper demonstrate that the decay and fluorescence spectral features of the bound 3,6-diaminoacridine derivatives are quite different from those of the bound 9AA in which three-exponential decays and zero quantum yield upon binding to poly(dG)·poly(dC) are observed [17]. This result may arise from differences between quenching interactions for 9AA and 3,6-diaminoacridine derivatives. It is clear that the GC pair has quenching ability in the order: 9AA > class I > class II. Even a small change in the dye structure may exert a large effect upon the binding interaction of the dye with DNA, reflecting changes in the electronic charge of the acridine ring or its amino groups [33,43] and in the geometry of the intercalated complex [44]. As is seen in table 3, the k_q value decreases in the order: PF-BZ < AF < PF for class I and BF < AY-ME < AY for class II. This result can be interpreted to indicate that the more bulky substituent attached to the acridine ring results in less favorable geometry between the dye and guanine residues so that efficient quenching does not occur. It is evident that the mechanism of the binding interaction does not have to be exactly the same for each dye. In fact, the finding that different intercalating dyes have different effects on the DNA structure suggests such a possibility [44]. Further, recent relaxation kinetic studies also show that the binding mechanism is rather complicated depending on the dye structure (ref. 45; and Kubota et al., unpublished results). Finally, it may be that transient fluorescence techniques can be used to indicate the heterogeneity of the binding sites in other aminoacridines.

References

1 A.R. Peacocke, in: Heterocyclic compounds: acridines, Vol. 9, ed. R.M. Acheson (Interscience, New York, 1973) p. 723.
2 E.R. Lochmann, and A. Micheler, in: Physico-chemical properties of nucleic acids, Vol. 1, ed. J. Duchesne (Academic Press, New York, 1973) p. 223.
3 S. Georghiou, Photochem. Photobiol. 26 (1977) 59.
4 G. Löber, J. Lumin. 22 (1981) 221.
5 A.R. Peacocke and J.N.H. Skerrett, Trans. Faraday Soc. 52 (1956) 261.
6 L.S. Lerman, J. Mol. Biol. 3 (1961) 18.
7 L.S. Lerman, Proc. Natl. Acad. Sci. U.S.A. 49 (1963) 94.
8 F.H.C. Crick, L. Barnett, S. Brenner and R.J. Watts-Tobin, Nature 192 (1961) 1227.
9 B.N. Ames, F.D. Lee and W.E. Durston, Proc. Natl. Acad. Sci. U.S.A. 70 (1973) 782.
10 A. Orgel and S. Brenner, J. Mol. Biol. 3 (1961) 762.
11 L.M. Chan and J.H. McCarter, Biochim. Biophys. Acta 204 (1970) 252.
12 U. Pachman and R. Rigler, Exp. Cell Res. 72 (1972) 602.
13 Y. Kubota, Chem. Lett. (1973) 299.
14 J.P. Schreiber and M. Daune, J. Mol. Biol. 83 (1974) 487.
15 S. Georghiou, Photochem. Photobiol. 22 (1975) 103.
16 Y. Kubota, K. Hirano and Y. Motoda, Chem. Lett. (1978) 123.
17 Y. Kubota and Y. Motoda, Biochemistry 19 (1980) 4189.
18 J. Reuben, B.M. Baker and N.R. Kallenbach, Biochemistry 17 (1978) 2915.
19 P.R. Young and N.R. Kallenbach, J. Mol. Biol. 145 (1981) 785.
20 C.H. Browning, J.B. Cohen, R. Gaunt and R. Gulbransen, J. Pathol. Bacteriol. 25 (1922) 329.
21 F. Ullmann and A. Marić, Chem. Ber. 34 (1901) 4307.
22 M. Shinitzky, J. Chem. Phys. 56 (1972) 229.
23 A. Grinvald and I.Z. Steinberg, Anal. Biochem. 59 (1974) 583.
24 A. Gafni, R.L. Modlin and L. Brand, Biophys. J. 15 (1975) 263.
25 P.R. Bevington, in: Data reduction and error analysis for the physical sciences (McGraw-Hill, New York, 1969) p. 187.
26 R.W. Armstrong, T. Kurucsev and U.P. Strauss, J. Am. Chem. Soc. 92 (1970) 3174.
27 E. Fredericq and C. Houssier, Biopolymers 11 (1972) 2281.
28 D. Fornaslero and T. Kurucsev, J. Phys. Chem. 85 (1981) 613.
29 R.K. Tubbs, W.E. Ditmars and Q. Van Winkle, J. Mol. Biol. 9 (1964) 545.
30 Y. Kubota and R.F. Steiner, Biophys. Chem. 6 (1977) 279.
31 G. Duportail, Y. Mauss and J. Chambron, Biopolymers 16 (1977) 1397.
32 P. Wahl, J.C. Auchet and B. Donzel, Rev. Sci. Instrum. 45 (1974) 28.
33 M.G. Badea and S. Georghiou, Photochem. Photobiol. 24 (1976) 417.
34 Y. Kubota and Y. Motoda, J. Phys. Chem. 84 (1980) 2855.
35 C.A. Parker, in: Photoluminescence of solutions (Elsevier, Amsterdam, 1968) p. 74.
36 M.H. Hui and W.R. Ware, J. Am. Chem. Soc. 98 (1976) 4712.
37 H.J. Li and D.M. Crothers, J. Mol. Biol. 39 (1969) 461.
38 J. Ramstein and M. Leng, Biophys. Chem. 3 (1975) 234.
39 M. Dourlent and J.F. Hogrel, Biochemistry 15 (1976) 430.
40 J. Ramstein, M. Ehrenberg and R. Rigler, Biochemistry 19 (1980) 3938.
41 T.D. Sakore, S.C. Jain, C.C. Tsai and H.M. Sobell, Proc. Natl. Acad. Sci. U.S.A. 74 (1977) 188.

42 S. Neidle, A. Achari, G.L. Taylor, H.M. Berman, H.L. Carrell, J.P. Glusker and W.C. Stallings, Nature 269 (1977) 304.
43 L.L. Ingraham and H. Johansen, Arch. Biochem. Biophys. 132 (1969) 205.
44 M. Hogan, N. Dattagupta and D.M. Crothers, Biochemistry 18 (1979) 280.
45 L.P.G. Wakelin and M.J. Waring, J. Mol. Biol. 144 (1980) 183.